

MPIH - V32 - 1996  
hep-ph/9607474

## Baryon Asymmetry of the Proton Sea at Low $x$

Boris Kopeliovich\* and Bogdan Povh†

*Max-Planck Institut für Kernphysik, Postfach 103980, 69029 Heidelberg, Germany*

### Abstract

We predict a nonvanishing baryon asymmetry of the proton sea at low  $x$ . It is expected to be about 7% and nearly  $x$ -independent at  $x < 0.5 \times 10^{-3}$ . The asymmetry arises from the baryon-antibaryon component of the Pomeron, rather than from the valence quarks of the proton, which are widely believed carriers of baryon number. Experimental study of  $x$ -distribution of the baryon asymmetry of the proton sea can be performed in  $ep$  or  $\gamma p$  interactions at HERA, where  $x \sim 10^{-5}$  are reachable, smaller than at any of existing or planned proton colliders.

---

\*On leave of absence from Joint Institute for Nuclear Research, Laboratory of Nuclear Problems, Dubna, 141980 Moscow Region, Russia. E-mail: bzk@dxnhd1.mpi-hd.mpg.de

†E-mail: povh@dxnhd1.mpi-hd.mpg.de

## 1. Introduction

The carrier of the baryon identity, the baryon number (BN) is defined rather loosely in most of the hadronic models, with a possible exception of the color string model. In this paper we consider the partonic treatment of BN.

One can prescribe  $BN = \pm 1/3$  to each quark or antiquark. In this case BN asymmetry is a direct consequence of the quark-antiquark asymmetry or vice versa. Then the question arises, how can BN of the proton find itself down at low  $x$ ? The simplest and wide spread prejudice is, that BN is carried only by the valence quarks. This means that in order to find the proton BN at low  $x$  one should slow down at least one of the valence quarks to low  $x$ . An example is shown schematically in Fig. 1a, where a vertical axis is assumed to correspond to Bjorken  $x$ . This mechanism provides BN with the same distribution  $\propto 1/\sqrt{x}$  as for valence quarks.

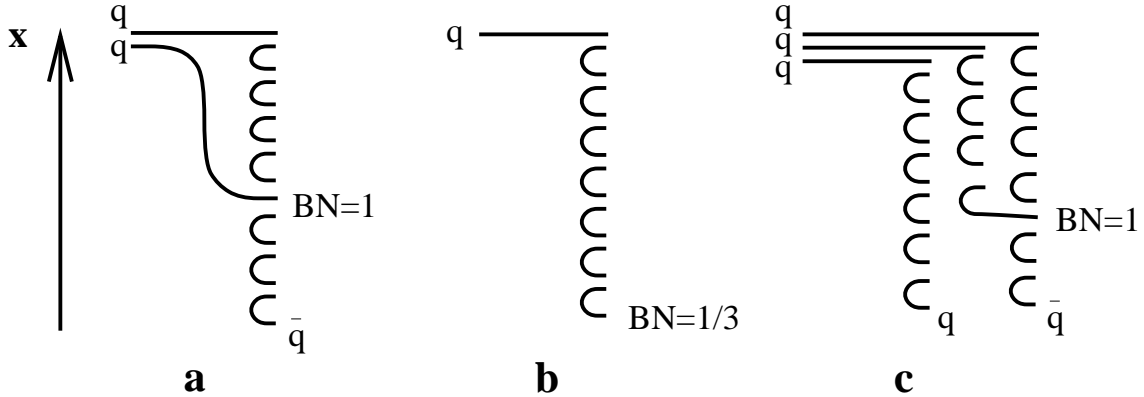


Figure 1: *Different mechanisms of BN flow down to low  $x$ .* **a:** The valence quark itself is slowed down. **b:** The valence quark surrounded by a sea-parton cloud. BN flows down to low  $x$  through the  $q\bar{q}$  chain. **c:** Three valence quarks in a decuplet-color state develop three  $q\bar{q}$  chains, which carry the BN. Conventionally we assume a vertical  $x$ -axis.

There is, however, another way to transport the  $BN = 1/3$  of the valence quark down to low  $x$  through a chain of sea quarks - antiquarks as is illustrated in Fig. 1b. Since the chain is BN-symmetric, except the very last quark at low  $x$ , the valence BN finds itself at low  $x$ . It is natural that in this case the BN has the same distribution  $\sim 1/x$  as the sea

quarks.

An important difference from the previous example in Fig. 1a is that there is no correlation between the flavour of the low- $x$  quark carrying the BN and the flavour of the valence quark initiating the chain. In this sense one may say that not only the valence quark itself, but the  $q - \bar{q}$  chain carries the BN as well.

However, the two other valence quarks in the proton (in any baryon) are mostly in a color-antitriplet state and develop their own  $q\bar{q}$  chain, but of an opposite alignment: anti-BN  $-1/3$  is transported down to low  $x$ , where it compensates exactly the BN of the sea of the first valence quark. This fact makes it difficult to realize the mechanism of BN flow shown in Fig. 1b.

There is, however, a probability to find two valence quarks in the proton in a sextet-color state. It may happen in the higher Fock components of the proton, for instance in  $|uudgg\rangle$ . The two additional gluons can be in different color-states, a singlet, two octets and an antidecuplet. In the latter case any of the two valence quarks are in a color-sextet state, i.e. each of the valence quarks develops its own sea  $q\bar{q}$  chain and transports its BN to low  $x$  as illustrated in Fig. 1c, where the gluons responsible for color conservation are not shown. We estimate the probability of such a configuration below.

One can interpret these results in terms of string model as well. In this approach baryons are assumed to have a Y-star configuration. This suggests to relate BN with the string junction, the point where the three strings join [1]. In this case BN is carried by gluonic field rather than by the valence quarks at the endpoints of the strings. Indeed, if the baryon is excited, each of the strings may break due to  $q\bar{q}$  pair production. In this case the valence quarks split away as mesons, but eventually a baryon is produced around the same string junction.

Such a star-structure of baryon naturally arises as a string analogue to the locally gauge-invariant operator with  $BN = 1$  [1]

$$|3q^v\rangle = J^{i_1 i_2 i_3}(X) G_{i_1}^{j_1}[P(X, X_1)] G_{i_2}^{j_2}[P(X, X_2)] G_{i_3}^{j_3}[P(X, X_3)] \times$$

$$q_{j_1}^v(X_1)q_{j_2}^v(X_2)q_{j_3}^v(X_3) , \quad (1)$$

where

$$G_i^j[P(X, X')] = \left[ T \exp \left\{ ig \int_{P(X, X')} A_\mu(X) dX^\mu \right\} \right]_i^j \quad (2)$$

the integration goes along path  $P(X, X')$  between points  $X$  and  $X'$ . Tensor  $J^{i_1, i_2, i_3}(X)$  should be associated with string junction  $J$  having coordinate  $X$  as is illustrated in Fig. 2a.

As soon as the string junction shares the proton momentum it is reasonable to provide it with a partonic interpretation. Let us consider the Fock-state decomposition of the light-cone wave function of the proton.

$$|p\rangle = |3q^v\rangle + |3q^v q^s \bar{q}^s\rangle + |3q^v 2q^s 2\bar{q}^s\rangle + \dots \quad (3)$$

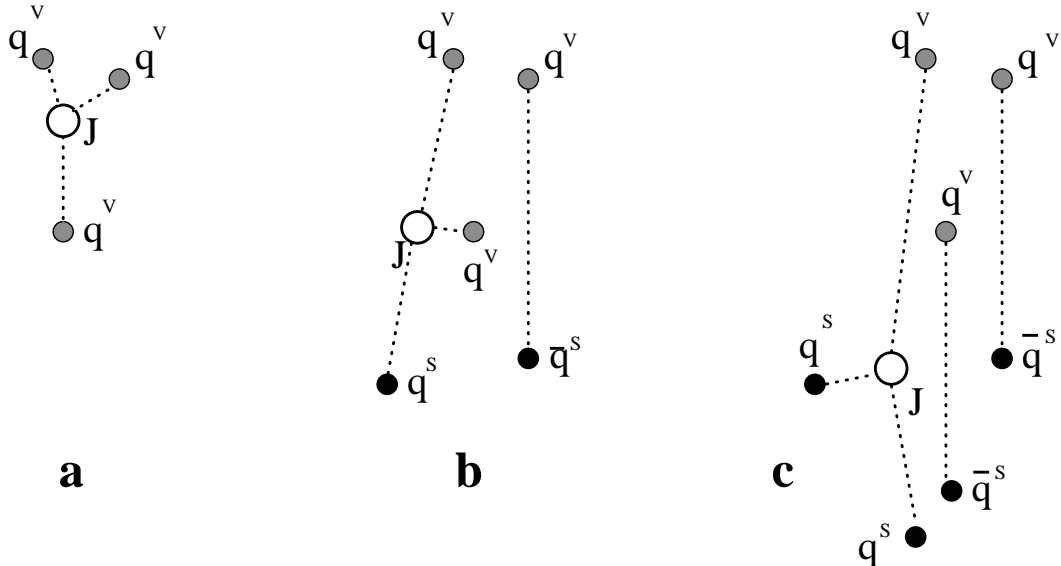


Figure 2: The cartoon shows the string configurations which correspond to different terms in Fock state decomposition (3). Grey and black circles show the valence and sea quarks respectively. The open circles show the position of the string junction. The dotted lines correspond to triplet color strings. Conventionally we assume a vertical  $x$ -axis.

The first term of (3) corresponds to expression (1) and is presented in Fig. 2a. In order to move the string junction down to lower  $x$  one should slow down at least two of the three

valence quarks. We assume dominance of a minimum energy configuration of the strings, what makes the string junction to follow the diquark rather than a single quark. Thus, the probability to find the string junction at low  $x$  in this Fock state is

$$B_1(x) \propto \frac{1}{x^{\alpha^0(M_4^J)}} , \quad (4)$$

where  $\alpha^0(M_4^J)$  is the intercept of the Regge trajectory corresponding to diquark-antidiquark mesons ( $M_4^J$ ) according to the classification and notations in [1]) shown schematically in Fig. 3a.

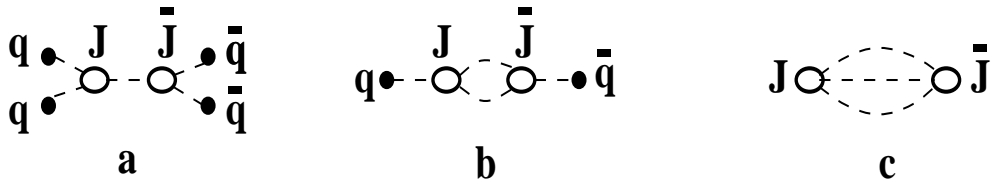


Figure 3: *Mesonic states (notations from [1]) lying on the Regge trajectories giving rise to BN exchange.* **a:** The diquark-antidiquark meson  $M_4^J$ . **b:** The  $qJ - \bar{q}\bar{J}$  meson  $M_2^J$ . **c:** The  $J - \bar{J}$  glueball meson  $M_0^J$ .

It is related to known parameters of other Reggeons,

$$\alpha^0(M_4^J) = 2\alpha_N^0 - \alpha_\rho^0 \approx -1.2 , \quad (5)$$

where  $\alpha_N \approx -0.4$  and  $\alpha_\rho \approx 0.5$  are the intercepts of the nucleon and  $\rho$ -meson trajectories. Although relation (5) was first derived in [2] using an oversimplified multiperipheral model, it also follows from the factorization relations of [3] for planar graphs (see also review [4]).

The second Fock component in (3) can be split into two colorless clusters, a  $3q$ -star and  $q\bar{q}$  color dipole. The corresponding wave function reads

$$\begin{aligned} |3q^v q^s \bar{q}^s\rangle &= q_{j_1}^v(X_1) G_{i_1}^{j_1}[P(X, X_1)] J^{i_1 i_2 i_3}(X) G_{i_2}^{j_2}[P(X, X_2)] q_{j_2}^v(X_2) G_{i_3}^{j_3}[P(X, X_3)] q_{j_3}^s(X_4) \\ &\quad \bar{q}^{sm}(X_5) G_m^l[P(X_3, X_5)] q_l^v(X_3) , \end{aligned} \quad (6)$$

where we have chosen the case when the dipole contains the valence quark and the sea antiquark. Of course such a specific color distribution may be suppressed by a color factor, which affects only the probability, but not the  $x$ -dependence. The string configuration corresponding to the wave function (6) is shown in Fig. 2b. The minimum energy string star in the  $|2q^v q^s\rangle$  state corresponds to the string junction having nearly the same  $x$  as the slowest of the valence quark. This is shown in Fig. 2b, where we assume conventionally a vertical  $x$ -axes.

Thus we come to the conclusion that the 5-quark Fock component of the proton light-cone wave function provides a low- $x$  distribution of the string junction which follows that for the valence quarks, i.e.  $\sim 1/\sqrt{x}$ .

On the other hand, the low- $x$  behaviour of the string junction accompanied by a valence quark corresponds to the intercept of the Regge trajectory for the  $qJ - \bar{J}\bar{q}$  states ( $M_2^J$  in notations of [1]) shown in Fig. 3b.

$$B_2(x) \propto \frac{1}{x^{\alpha^0(M_2^J)}} . \quad (7)$$

We conclude from the above consideration that

$$\alpha^0(M_2^J) = \frac{1}{2} . \quad (8)$$

This value of the intercept first claimed in [5, 6], is higher than one suggested in [2, 1] on the basis of an oversimplified multiperipheral bootstrap model. There are, however, a few experimental confirmations of the value given in (8).

- It is demonstrated in [6] that (8) is in perfect agreement with the energy dependence of the data [7, 8, 9] on BN number production in the central rapidity region in  $pp$  collisions. The absolute value of the cross section evaluated in perturbative QCD in [6] agrees with the data as well. Below we present a new calculation, which does not rely upon pQCD.
- Evaluation of the  $\bar{p}p$  annihilation cross section [5] assuming dominance of the  $M_2^J$

Reggeon exchange is in a good agreement with available (up to 12  $GeV$ ) data. The value of the intercept eq. (8) naturally explains the observed energy dependence  $\sigma_{ann}^{p\bar{p}} \propto 1/\sqrt{s}$ .

- The dynamics of the  $M_2^J$  Reggeon exchange was applied recently [10] to BN stopping in high-energy heavy ion collisions. It was found to be a dominant mechanism for net BN production at mid rapidities at 200  $GeV$  and nicely explains the data from the NA35 experiment [11] on S-S collisions. The predicted baryon stopping in Pb-Pb collisions [10] was confirmed recently by data [12] at 158  $GeV$ .

The *third* term in eq. (3) is illustrated in Fig. 2c, where we again include a valence quark and a sea antiquark in each color dipole. The wave function of this Fock component reads

$$|3q^v 2q^s 2\bar{q}^s\rangle = q_{j_1}^v(X_1) G_{i_1}^{j_1}[P(X, X_1)] J^{i_1 i_2 i_3}(X) G_{i_2}^{j_2}[P(X, X_2)] q_{j_2}^s(X_4) G_{i_3}^{j_3}[P(X, X_3)] q_{j_3}^s(X_6) \times \bar{q}^{sm}(X_5) G_m^l[P(X_2, X_5)] q_l^v(X_2) \bar{q}^{sm}(X_7) G_m^l[P(X_3, X_7)] q_l^v(X_3) \quad (9)$$

We again assume that the sea quarks have smaller  $x$ -values than the valence ones, as is indicated in Fig. 2c. The minimum energy of the string configuration is reached when the string junction has nearly the same  $x$  as that of the two sea quarks. Consequently, the string junction, i.e. BN, has in the third term of Fock decomposition (3) the same  $x$ -distribution  $\sim 1/x$  as the sea quarks.

This important conclusion means that the Regge trajectory corresponding to the  $J - \bar{J}$  mesons (Fig. 3c)  $M_0^J$  (notation of [1]) and providing  $x$ -distribution of BN

$$B_3(x) \propto \frac{1}{x^{\alpha^0(M_0^J)}} , \quad (10)$$

has intercept

$$\alpha^0(M_0^J) = 1 . \quad (11)$$

Thus, we arrived at the same conclusion as we drew from the consideration of the  $q\bar{q}$  chains shown in Fig. 1. This result (11) also follows from energy independence of the  $\bar{p}p$  annihilation

cross section claimed in [17], where it was assumed that BN annihilation results from overlap of the string junction and antijunction in impact parameter plane. It was guessed in analogy with inelastic reactions initiated by crossing of the strings, that the string rearrangement in annihilation is also energy independent. The authors of [17] estimated also the asymptotic annihilation cross section at  $\sigma_{ann}^{\bar{p}p} \approx 1 - 2 \text{ mb}$ .

Perturbative QCD calculations [13, 14, 15, 16] of the annihilation via two-gluon exchange proved energy-independence of the cross section. Moreover, even the absolute value of asymptotic annihilation cross section was predicted in a parameter-free way to be the same,  $1 - 2 \text{ mb}$ , as in [17].

The annihilation cross section is measured only up to  $12 \text{ GeV}$ , and it is not very likely to get data at much higher energies. Nevertheless, a solid confirmation of the above predictions was found in [5] from an analysis of particle multiplicity distribution in  $\bar{p}p$  and  $p\bar{p}$  interactions at high energies. The string junction exchange, or its perturbative analogue the color-decuplet gluonic exchange [13]-[15] lead to a three-sheet topology of final state (see Fig. 1c). This implies a high multiplicity of produced particles, about  $3/2$  of the mean multiplicity. Such a signature allows to single out a pure string junction exchange. Analysis [15] of available data on multiplicity distribution confirms the energy independence of the cross section with value  $\sigma_{ann}^{\bar{p}p} = 1.5 \pm 0.1 \text{ mb}$  in a perfect agreement with the theoretical predictions [17, 14, 15]

Note that these theoretical and experimental results are in variance with the expectation of [2, 1] that  $\alpha^0(M_0^J) = 1/2$ .

Summarizing, we expect the BN density distribution in the proton to have the form

$$B_p(x) - \bar{B}_p(x) = \sum_{k=0}^2 C_{2k} x^{-\alpha(M_{2k}^J)} \quad (12)$$

We subtract the anti-BN density in order to remove the trivial baryon symmetric part of the sea. The sum rule representing BN conservation demands

$$\int_{x_{min}}^1 dx \left[ B_p(x) - \bar{B}_p(x) \right] = 1 , \quad (13)$$

where  $x_{min} = Q^2/2m_N\nu$  or  $m_N/\nu$  for virtual or real photons, respectively.

In the present paper we suggest an experimental study of the BN distribution at low  $x$  in  $ep$  or  $\gamma p$  interactions at HERA. In order to study the momentum distribution of the produced net BN one should measure the difference between the baryon ( $B$ ) and antibaryon ( $\bar{B}$ ) production rates. Such a net BN distribution reflexes the  $x$ -distribution of the string junction in the projectile proton, since the final state baryon is produced with nearly the same  $x$ . Note that  $x$  is defined as a ratio of the final baryon to the initial proton light-cone momenta,  $x = p_B^+/p_p^+$ , but not through the virtuality and the energy of the photon. We predict  $d\sigma(\gamma^*p \rightarrow BX)/dx \propto 1/\sqrt{x}$  at  $x > 5 \times 10^{-4}$  and asymptotic behaviour,  $d\sigma(\gamma^*p \rightarrow BX)/dx \propto 1/x$  at smaller  $x$ . HERA seems to be the best machine for such studies, since it provides the smallest values of  $x$  compared to any of planned proton colliders, RHIC, LHC or even SSC would have reached.

We discuss the ways to probe the baryon asymmetry of the sea in the next section. We demonstrate that usual probe of the quark/antiquark asymmetry cannot be used at low  $x$  and suggest to measure the baryon asymmetry of produced particles.

In section 3 we discuss and provide a numerical evaluation of the gluonic contribution to the baryon asymmetry, which dominates at very low  $x$ .

The valence quark contribution to the baryon asymmetry, which is important down to quite low  $x$ , is evaluated in section 4.

In section 5 we estimate unitarity corrections to BN distribution, which may be important at high energies. We found a 20% correction for the energy of HERA.

## 2. How to probe the baryon asymmetry?

BN, like gluons, cannot be directly probed by a virtual photon, and one should look for other probes.

A baryon asymmetry of the sea obviously manifests itself in the quark/antiquark asym-

metry. The latter was suggested in [18] to be measured in deep-inelastic neutrino interactions, which are different for quarks and antiquarks. This method, however, cannot be used to measure the low- $x$  baryon asymmetry under discussion. Indeed, the color string configuration shown in Fig. 2c is quark/antiquark symmetric at low  $x$ , in spite of the presence of the string junction (the  $q/\bar{q}$  asymmetry appears as a result of hadronization of the strings). A high-energy neutrino, which develops a  $q_1\bar{q}_2$  ( $u\bar{d}$ ,  $c\bar{s}\dots$ ) fluctuation through the  $W$ -boson, interacts with this string configuration with the same cross section as an antineutrino, as far as the valence quark of the proton are not involved in the interaction. Thus, it is insensitive to a baryon asymmetry. The same can be demonstrated in the quark-chain representation illustrated in Fig. 1c. As for  $u\bar{d}$  and  $\bar{u}d$  fluctuations, the  $\nu/\bar{\nu}$  symmetry is obvious (provided that isospin symmetry of the sea at low  $x$  is true). There is no symmetry, however, for strange quarks. Since strangeness is conserved, its distribution has a maximum at the rapidity of the string junction, and a negative minimum in the vicinity in the  $x$ -scale. Such an oscillation causes a complete cancellation of the strangeness at a fixed value of  $x$ , probed by the neutrino, when one averages over the  $x$ -value of the baryon. This cancellation does not take place in the case of quark/antiquark asymmetry generated by  $K\Lambda$  Fock component of the proton considered in [18].

Searching for another signature of BN one can use the shortness of rapidity-correlations between the primordial BN and the produced baryon, typical for all known models of hadronization. Therefore, we assume that the  $x$ -distribution of the produced baryon is close to the primordial BN distribution. Of course the baryon-antibaryon pairs spontaneously produced from vacuum also contribute, but this background can be eliminated by subtraction of baryon and antibaryon production rates. We define the baryon/antibaryon production asymmetry as

$$A_B(x) = \frac{\Delta_B(x)}{\Sigma_B(x)} . \quad (14)$$

Here we denote  $\Delta_B(x) = N_B(x) - N_{\bar{B}}(x)$  and  $\Sigma_B(x) = [N_B(x) + N_{\bar{B}}(x)]/2$ , where  $N_B(x) = [xd\sigma(B)/dx]/\sigma_{in}$  is the ratio of the inclusive (anti)baryon production to the total inelastic

cross sections.

### 3. Gluonic contribution to the BN density at low $x$

Thus, the observable reflecting the BN distribution in the proton is the baryon asymmetry (14) of produced particles. It should be pointed out that partonic interpretation is not Lorentz invariant and may look quite differently depending on the reference frame. For example, one cannot say to which one of the two colliding hadrons the sea parton belongs, as the answer depends on the reference frame. Even a valence quark of one colliding hadron may look in the rest frame of this hadron as a sea quark of another one.

The same is true for the partonic interpretation of the BN distribution in the proton. The Lorentz-invariant observable, the baryon asymmetry of the produced particles can be calculated, of course, in any reference frame. It is, however, most convenient to do the estimation in the proton rest frame, since one can use available information on the BN annihilation cross section at high energies, which we mentioned in the introduction. In this reference frame the produced BN is supposed to preexist as a fluctuation of the photon, accompanied by an anti-BN, due to BN conservation. The latter has to annihilate with the BN of the target in order to produce the observed baryon asymmetry. Two examples are sketched in Fig. 4.

The amount of the sea  $B\bar{B}$  pairs stored in the photon fluctuation cancels in the relative asymmetry (14), and we arrive at a very simple expression for the baryon asymmetry

$$A_B(x) = \frac{\sigma_{ann}^{B\bar{B}}(s = m_N^2/x)}{\sigma_{in}^{hp}} , \quad (15)$$

which is very important for further applications. Here  $\sigma_{in}^{hp}$  is the inelastic cross section for the dominant hadronic fluctuation of the photon at  $s = m_N^2/x$ . It is the  $\rho$ -meson in the case of a real photon, so we will use  $\sigma_{in}^{hp} \approx 20 \text{ mb}$ . We do not expect any strong  $Q^2$ -dependence of the baryon asymmetry, despite the fact that the photoabsorption cross section for highly virtual photons decreases as  $1/Q^2$ . This may be interpreted as a suppression  $\sim 1/Q^2$  of interaction of small-size,  $\propto 1/Q^2$ , fluctuations of the photon. At the same time the baryon-

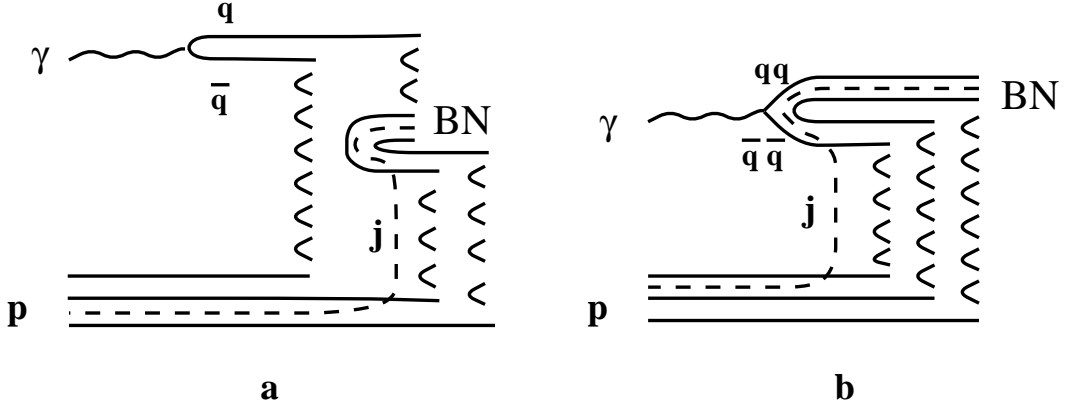


Figure 4: *Gluonic mechanism of the proton BN flow to the central rapidity region (a) and to the photon fragmentation region (b).* The dashed lines show the trajectory of the string junction

antibaryon component of these fluctuations has to have a small transverse separation as well. Thus the annihilation cross section acquires the same suppression factor  $1/Q^2$ .

In order to proceed further with the evaluation of the baryon asymmetry (15) one needs to know the baryon-antibaryon annihilation cross section  $\sigma_{ann}^{B\bar{B}}$  at high energies. As mentioned in the introduction, the asymptotic behaviour of the annihilation cross section was studied in nonperturbative [17] and perturbative [14, 16] QCD approaches, and also analysing data on multiplicity distribution in  $pp$  and  $p\bar{p}$  interactions [15, 16]. Using so different ideas all these approaches arrive at the same conclusion: the annihilation cross section at high energies is about  $1 - 2 \text{ mb}$  and nearly energy-independent.

Using (15) we find  $x$ -independent baryon asymmetry  $A_B^0 \approx 7\%$ . This asymmetry is due to flow of the BN of the initial proton traced by the gluons.

We can also estimate the absolute value of the yield of the net BN  $\Delta_B(x)$  provided that the total yield of baryons is known. Baryon-antibaryon pair production from vacuum is known to be substantially suppressed compared to mesons [19, 20, 21],  $\Sigma_B(x) = \epsilon N_\pi(x)$ , where  $\epsilon \approx 0.08$  and  $N_\pi(x) = [xd\sigma(\pi)/dx]/\sigma_{in} \approx 3 - 5$  [22], dependent on energy. Then eq. (15) leads to the estimate

$$\Delta_B(x) \approx \epsilon \frac{\sigma_{ann}}{\sigma_{in}^{hp}} N_\pi(x) \approx 0.02 . \quad (16)$$

Thus, only about 2% of the total photoabsorption cross section goes for production of net BN per unit of rapidity.

The realistic rapidity distribution of particle production is nearly constant only in the central region, but decreases towards the rapidity of the projectile. Thus, eq. (16) may overestimate baryon production in the photon fragmentation region. On the other hand, there is a specific channel of BN production by means of a spontaneous dissociation of the photon into the diquark-antidiquark pair. The anti-string-junction may subsequently annihilate with the string junction of the proton, as sketched in Fig. 4b.

To evaluate the cross section of the net BN production in the photon fragmentation region we take into account the suppression by factor of  $\sim 0.08$  for the diquark compared to a quark pair production, and the smallness of annihilation compared to the total inelastic cross section,  $\sigma_{ann}/\sigma_{in}^{hp} \approx 0.07$ . Therefore, in 0.6% of all DIS events the net BN is produced by the photon dissociation mechanism. The corresponding contribution to the inclusive cross section  $d\sigma(B - \bar{B})/dy \propto \exp(y - y_\gamma)$  peaks at the photon rapidity  $y_\gamma$ .

Thus, the gluonic mechanism of BN transfer predicts a plateau for net BN distribution at mid rapidities and a peak in the photon fragmentation region.

#### 4. Valence quark contribution to the BN distribution

We expect a substantial growth of the baryon asymmetry towards the proton fragmentation region due to the quark mechanism of BN transfer [6]. On the other hand, it may extend down to quite low  $x$ . Perturbative calculation of the BN flow over large rapidity intervals performed in [6] is in a good agreement with the measurement of the baryon asymmetry in central rapidity region measured in  $pp$  interaction at ISR [7]. The  $x$ -dependence of this mechanism is controlled according to (7) – (8) by the leading Reggeon intercept,  $\alpha_R(0) = 1/2$ , so one can write [6]

$$\Delta_B^{(q)} = \delta_q \sqrt{x} . \quad (17)$$

The factor  $\delta_q$  can be either borrowed from the calculations [6], or fixed by comparison with available data [7, 8, 9], which gives  $\delta_q \approx 0.6$ . Assuming that  $\sigma_{in}^{pp} \approx 1.5 \sigma_{in}^{\pi p}$  we get  $\delta_q \approx 1$

One can also evaluate the contribution of the valence quarks to the baryon asymmetry using same equation (15) except the annihilation cross section is to be evaluated within the same quark mechanism of BN transfer as it was done in [5], or one can use directly the data on annihilation cross section at preasymptotic energies,  $\sigma_{ann}^{p\bar{p}} \approx 70 \text{ mb } \sqrt{s_0/s}$ . Thus, (15) gives similar value  $\Delta_q \approx 1.1$ .

The calculated baryon asymmetry

$$A_B(\eta) = \frac{\Delta_B^{(q)}(\eta)}{\Delta_B^{(q)}(\eta) + \epsilon N_\pi(\eta)} , \quad (18)$$

is plotted in Fig. 5 as function of the baryon rapidity  $\eta = \eta_p - \ln(1/x)$  in the laboratory frame. From this figure we expect that the gluonic mechanism dominates at  $\eta < -1$  at HERA.

## 5. The BN conservation sum rule. Unitarity corrections.

In spite of the smallness of the baryon asymmetry it comes to a contradiction with the BN conservation sum rule eq. (13) at very low  $x$  if  $A_B(x) = A_B^0$  is a constant. Indeed, relation (13) for BN distribution can be rewritten for the baryon asymmetry using (14) as

$$\int_{x_{min}}^1 \frac{dx}{x} A_B(x) \Sigma_B(x) = 1 , \quad (19)$$

but the left-hand side of this relation grows with  $1/x$  since  $\Sigma_B(x) \approx \epsilon N_\pi(x)$  and

$$\int_{x_{min}}^1 \frac{dx}{x} A_B(x) N_\pi(x) > A_B^0 \langle N_\pi \rangle , \quad (20)$$

where  $\langle N_\pi \rangle = \int dx/x N_\pi(x)$  is the mean multiplicity of produced pions, which is known to grow as  $1/x^{\alpha_P-1}$  if the Pomeron intercept  $\alpha_P > 1$ , or as  $\ln(1/x)$  for  $\alpha_P = 1$ . In any case the

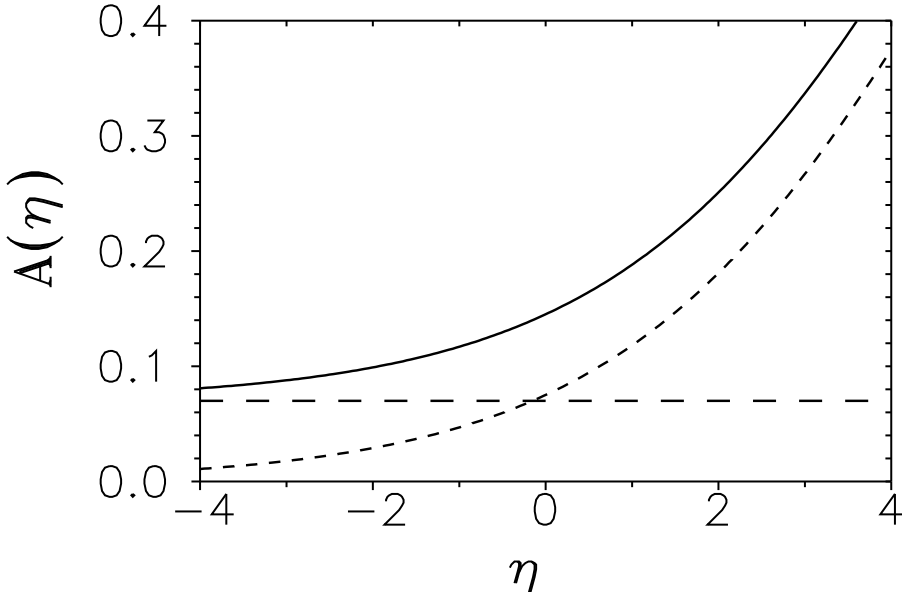


Figure 5: *Baryon asymmetry in  $\gamma p$  interaction at HERA versus rapidity in the laboratory frame. The dashed line corresponds to the rapidity-independent gluonic mechanism of BN transfer. The dotted curve represents the quark mechanism of BN transfer, calculated with (17)-(18). The solid curve is the sum of the two contributions.*

sum rule eq. (19) is violated.

The source of the puzzle can be understood as follows. Following section 3 we treat the baryon asymmetry as a result of creation of a sea baryon-antibaryon fluctuation in the projectile photon and annihilation of the antibaryon with the target proton. This mechanism leads to the basic relation Eq. (15). Although the probability of a  $B\bar{B}$  fluctuation is strongly suppressed by the smallness of the factor  $\epsilon$ , the number of such pairs grow with  $1/x$ , and the amount of  $B\bar{B}$  pairs in a photon fluctuation becomes eventually large at very low  $x$ . However, only one of these virtual  $\bar{B}$ s has a chance to annihilate with the target proton and create a baryon asymmetry with corresponding  $x$ . Thus, annihilation of different  $B\bar{B}$  pairs in the photon fluctuation shadow each other.

In order to take into account the growth of the integral in eq. (19) we should introduce unitarity correction and renormalize the BN flow

$$\tilde{\Delta}_B(x) = \Delta_B(x) \left[ \int_{x_{min}}^1 \frac{dx'}{x'} \Delta_B(x') \right]^{-1} \quad (21)$$

This expression obviously satisfy the sum rule eq. (19). It is easily interpreted: the total amount of the net BN, which flows down to low  $x$  is fixed, but phase space  $\ln(1/x_{min})$  where this BN can be distributed grows with energy. Therefore,  $\Delta_B(x)$  and  $A_B(x)$  must decrease with energy at fixed  $x$ , what is provided with the denominator in (21). Nevertheless, due to the smallness of the asymptotic value of BN flow estimated in (16) the unitarity correction (21) is quite small at presently available energies. For the biggest rapidity interval of HERA all the curves shown in Fig. 5 must be renormalized by about 20% down due to the unitarity corrections (21).

## 6. Discussion and conclusions.

A proton looks in its infinite-momentum frame like a cloud of partons, quarks, antiquarks and gluons. The question, how the BN of the proton is distributed in such a cloud is the main issue of the present paper. Our main observations are:

- BN of the proton can be carried either by the valence quarks or by the sea quarks and gluons. In the latter case BN is distributed like  $1/x$  down to very low  $x$ . We predict an unusual phenomenon, baryon asymmetry of the sea in the proton at very low  $x$ , which we estimate at  $A_B(x) \approx 0.07$ . This number reflects the admixture of the  $BN - \overline{BN}$  exchange in the Pomeron. Unitarity corrections suppress  $A_B(x)$  dependent on the rapidity interval of the  $\gamma^* p$  collision. This is 20% effect for the energy range of HERA.
- The BN distribution at medium  $x$  is provided by a single valence quark. It is the dominant contribution to the baryon asymmetry  $A_B(x) \approx 3/\sqrt{x}$  down to  $x \approx 5 \times 10^{-4}$ .
- The baryon asymmetry at the parton level can be observed through a baryon asymmetry of produced particles in proton interactions at high-energies. The smallest  $x \approx 10^{-5}$  can be reached in (virtual) photon - proton interactions at HERA.

An important ingredient of our consideration is the method, which is used for the calculation of the BN distribution. It is based on Lorenz-invariance of the observable baryon asymmetry, and allows one to replace the problem of BN distribution in the projectile proton by the rather well known process of annihilation of the primordial anti-BN with the target proton. In this way we derived eq. (14), which is the central result of the paper. Using it, we predicted the baryon asymmetry provided by the valence quarks and gluons, which is shown for kinematics of HERA in Fig. 5.

It is worth while reminding that the quark mechanism of BN transfer suggested in [6] is different and provides much larger baryon asymmetry than what follows from the baryon asymmetry in hadronization of a valence quark.

Although we use the ideas and the results of [13]-[16] and [5, 6], essentially based on perturbative QCD calculations, which applicability is questionable, our predictions are free of this uncertainty. In the case of the quark mechanism of BN transfer we use in (14) experimentally measured value of  $\sigma_{ann}^{p\bar{p}}$ . As for the gluonic mechanism, no direct measurement of baryon annihilation at high energies was done so far. However, we consider the asymptotic value of  $\sigma_{ann}^{p\bar{p}} \approx 1.5 \text{ mb}$  as a very reliable one, since it follows from the phenomenological analysis of data on multiparticle production [15], as well as from nonperturbative [17] and perturbative [14] QCD estimations.

Experimental study of BN transfer through the biggest rapidity interval was done so far at ISR [7, 8, 9]. It was a measurement of the difference of inclusive cross sections of  $p$  and  $\bar{p}$  produced in central rapidity region. The smallest value of  $x$  reached in this experiment was  $x \approx 10^{-2}$ . Unlike the proton colliders, one can use the whole rapidity interval with  $e - p$  colliders. At HERA it corresponds to  $x \approx 10^{-5}$ , which is smaller than at any of available or planned proton colliders.

We predict a flavour-independent baryon asymmetry. As for the absolute production rate, we do not expect the usual suppression of hyperon production compared with nucleons. This is because the produced baryons do not contain any light spectator quarks, but only string junctions. So, each of three quarks which joins the string junction to build up the

baryon may be either a strange quark or a light one. This provides a combinatorial factor of three, which essentially compensates the suppression for the strange quark production. This is confirmed by nearly the same branchings of  $J/\Psi$  decay into  $p\bar{p}$ ,  $\Sigma\bar{\Sigma}$  and  $\Xi\bar{\Xi}$  [22]. This decay proceeds through three gluons, which create a string junction-antijunction pair in final state, which then dresses up with  $u$ ,  $d$  or  $s$  quarks. Note that thanks to the kinematics of HERA the baryons we are interested in, which are produced not far from the photon fragmentation region, are not very energetic, what makes the identification easier. One can study the production asymmetry for  $\Lambda$ -hyperons, which may be easier identified.

**Acknowledgements:** We would like to thank E. Gabathuler, T. Greenshaw and D. Milstead for informing us on preliminary results of the H1 Collaboration on  $\Lambda\bar{\Lambda}$  production in DIS and H. Meyer for pointing out the role of the baryon junction in the decay of  $J/\Psi$ . We are grateful to A.W. Thomas for useful discussion and comments and to J. Pochodzalla, who read the manuscript and made valuable improving suggestions.

## References

- [1] G.C. Rossi and G. Veneziano, Nucl. Phys. **B123** (1977) 507; Phys. Rep. **63** (1980) 149
- [2] Y. Eylon and H. Harari, Nucl. Phys. **B80** (1974) 349
- [3] A.B. Kaidalov, Phys. Lett. **116B** (1982) 459
- [4] A. Capella, U. Sukhatme, C. I. Tan and J. Tran Thanh Van, Phys. Rep. **236** (1994) 225
- [5] B.Z. Kopeliovich and B.G. Zakharov, Sov. J. Nucl. Phys. **49** (1989) 674
- [6] B.Z. Kopeliovich and B.G. Zakharov, Z.Phys.C **43** (1989) 241
- [7] B. Alper et al., Nucl. Phys. **B100** (1975) 237
- [8] T. Akesson et al., Nucl. Phys. **B228** (1983) 409

- [9] L. Camilleri, Phys. Rep. **53** (1987) 144
- [10] A. Capella and B.Z. Kopeliovich, LPTHE96-01 and MPIH-V07-1996, hep-ph/9603279, to appear in Phys. Lett. B.
- [11] The NA35 Collaboration : H. Ströbele et al, Nucl. Phys. **A525** (1991) 59c.
- [12] The KLLM Collaboration, P. Deines-Jones et al., LSU HEA-SS-96-03
- [13] B.Z. Kopeliovich, Sov, J. Nucl. Phys.**45** (1987) 1078
- [14] B.Z. Kopeliovich and B.G. Zakharov, Sov. J. Nucl. Phys. **48** (1988) 136
- [15] B.Z. Kopeliovich and B.G. Zakharov, Phys. Lett. **211B** (1988) 221
- [16] B.Z. Kopeliovich and B.G. Zakharov, Sov. Phys. Particles and nuclei, **22** (1991) 140
- [17] E. Gotsman and S. Nussinov, Phys. Rev. **D 22** (1980) 624
- [18] S.J. Brodsky and B.-Q. Ma, SLAC-PUB-7126, hep-ph/9604393
- [19] A. Casher, H. Neubereger, S. Nussinov, Phys. Rev. **D20** (1979) 179.
- [20] V.V. Anisovich, M.N. Kobrinsky, J. Niyri and Yu. Shabelsky, in "Quark model in high-energy collisions", World Scientific, Singapour, 1985
- [21] M. Anselmino et al., Rev.Mod.Phys. **65** (1993) 1199
- [22] Review of particle properties, L. Montanet et al., Phys. Rev. **50D** (1994) 1175